Desalination and Water Treatment
www.deswater.com

doi: 10.5004/dwt.2019.23916

151 (2019) 307–314
May

Removal of Ag(I) from aqueous solution by thiourea-functionalized silica gel: experimental and theoretical study

Zhendong Zhang[a], Xingrong Liu[a], Ke Wang[b], Yuzhong Niu[a,*], Hou Chen[a], Liangjiu Bai[a], Zhongxin Xue[a]

[a]*School of Chemistry and Materials Science, Ludong University, Yantai 264025, China, Tel. +86 535 6696162; emails: niuyuzhong@ldu.edu.cn (Y. Niu), 584149616@qq.com (Z. Zhang), 982964427@qq.com (X. Liu), lduchenhou@l26.com (H. Chen), bailiangjiu@163.com (L. Bai), ldxuezx@126.com (Z. Xue)*
[b]*Marine Chemical Research Institute Co. Ltd, State Key Laboratory of Marine Coatings, Qingdao 266071, China, Tel. +86 532 85845879; email: wanghan624@163.com (K. Wang)*

Received 16 September 2018; Accepted 3 February 2019

ABSTRACT

Thiourea-functionalized silica gel (HO-SG-GPTS-TS and HE-SG-GPTS-TS) were synthesized by homogeneous and heterogeneous methods, respectively. The feasibility of the as-prepared adsorbents for the remove of Ag(I) from aqueous solution was systemically studied under different solution pH, contact time, temperature, and initial Ag(I) concentration. The adsorption capacity is found to depend on the solution pH and the maximum adsorption capacity is achieved at pH 6. Adsorption kinetic indicates the adsorption can reach equilibrium within 180 min. The adsorption follows pseudo-second order model and is controlled by film diffusion process. Adsorption isotherm shows that the adsorption capacity increases with the increase of initial Ag(I) concentration and temperature. The adsorption isotherm is suitable to be simulated by Langmuir model and is proceeded by chemical mechanism. Thermodynamic parameters suggest the adsorption is a spontaneous, endothermic, and entropy increased process. Density functional theory calculation reveals that the formation of chelates with Ag(I) by S and hydroxyl O atoms dominate the adsorption, and S atom is the main contributor.

Keywords: Thiourea; Silica gel; Ag(I); Adsorption; Density functional theory

1. Introduction

With the rapid development of industry, wastewater contains metal ions has been extensively discharged into the environment [1,2]. The metal ions are toxic and non- biodegradable, which can accumulate in biological system and cause terrible effects to public health and ecological safety [3–5]. Among these metals, Ag(I) is widely released from the fields of electronic industry, battery industry, aerospace industry, etc. The digest of Ag(I) may damage the liver, kidney, and respiratory system [6–8]. Therefore, it is urgent to remove Ag(I) from aqueous solution.

A number of methods including membrane separation, ion-exchange, solvent extraction, chemical precipitation, and adsorption have been used for the removal of metal ion from aqueous solution [6,7,9]. Adsorption is considered to be attractive method due to its low cost, simple operation, high efficiency, and flexible in the design of adsorbent to meet different requirement [1,4]. Therefore, various adsorbents such as activated carbon [10], chitosan [11], clay [12], silica gel [13], graphene oxide [14], and polymers [15,16] have been used for metal ion elimination. The design and fabrication of novel adsorbent with high efficiency is still an important issue for the remediation of metal ion pollution.

* Corresponding author.

Among the various adsorbents, silica gel have been widely used for the removal of Ag(I) due to its large surface area, tunable porous structure, excellent thermal and chemical stability, and feasible surface functionalization [17–19]. For example, Taheri et al. [20] synthesized mesoporous silica/dendrimer amines based on [1,3,5]-triazines for the selective removal of aqueous Ag (I). Hong et al. [21] reported the use of crown ether modified mesoporous silica for the adsorption of Ag(I) in trace level. Our group also fabricated silica gel supported sulfur-capped PAMAM dendrimers for the selective adsorption of Ag(I) from aqueous solution [13]. According to Hard and Soft Acids and Bases (HSAB) concept, sulfur and nitrogen functional groups display special binding affinity toward Ag(I) [22,23]. Thiourea- containing functional groups which contain sulfur and nitrogen atoms have been favorably employed to construct adsorbent for metal ion removal [16,24–26]. Thus, the fabrication of adsorbent with thiourea and silica gel is anticipated to have fascinating adsorption property for Ag(I) from aqueous solution. However, the majority of previous works mainly focused on the synthesis and application of thiourea-containing adsorbents, little attention has been paid to reveal the interaction mechanism and the contribution of different donor atoms during the adsorption. Therefore, it is of vital importance to reveal the interaction mechanism from the perspective of molecular level, which will facilitate the fabrication of efficient adsorbent for the targeted metal ion.

In our previous work, thiourea-functionalized silica gel (HO-SG-GPTS-TS and HE-SG-GPTS-TS) were prepared by homogeneous and heterogeneous methods, and used for the robust removal of Hg(II) from aqueous solution [27]. The aim of the present study is to investigate the feasibility of HO-SG-GPTS-TS and HE-SG-GPTS-TS for the effective removal of Ag(I) from aqueous solution. The effects of solution pH, contact time, temperature, and initial Ag(I) concentration on the adsorption were investigated, and the adsorption mechanism was revealed on the molecule level based on the results of experimental and theoretical calculation.

2. Experimental

2.1. Materials and methods

The synthetic procedures of HO-SG-GPTS-TS and HE-SG-GPTS-TS were similar to our previous report as described in Fig. 1 [27]. The stock solution of Ag(I) with concentration of 0.04 mol·L^{-1} was prepared by dissolving certain amount of $AgNO_3$ with distilled water. All the reagents used were all analytical grades and purchased from Sinopharm Chemical Reagent Co., Ltd., China. The concentration of Ag(I) before and after adsorption was measured by a VARIAN AA240 atomic adsorption spectrophotometer (AAS).

2.2. Saturated adsorption capacity for metal ions

The saturated adsorption capacity for metal ions was determined by the following procedure: about 20 mL 0.002 mol·L^{-1} metal ion solutions and 20 mg adsorbent were added into 100 mL flask. The suspension was shaken at 25°C for 12 h, and then the concentration of residual metal ion was detected by AAS. The adsorption capacity was calculated by Eq. (1).

$$q = \frac{(C_0 - C)V}{W} \tag{1}$$

where q (mmol·g^{-1}) is adsorption capacity; C_0 and C are the initial and equilibrium Ag(I) concentration (mmol·mL^{-1}); V (mL) is the volume of the solution, and W(g) is the adsorbent mass.

2.3. Effect of pH on the adsorption of Ag(I)

The effect of pH on the adsorption was performed by equipping 20 mg adsorbent to a series of 20 mL 0.002 mol·L^{-1} Ag(I) solution with different pH of 1, 2, 3, 4, 5, and 6, respectively. The adjustment of solution pH for 1 and 2 was achieved by HNO_3 solution, while that of pH 3–6 was adjusted by acetate/acetic acid buffer solution. The mixture was shaken for 12 h at 25°C and the concentration of Ag(I) was determined by AAS.

2.4. Adsorption kinetic for Ag(I)

Adsorption kinetic was carried out by batch method as follows: a series of flasks were charged with 20 mg adsorbent and 20 mL 0.002 mol·L^{-1} Ag(I) solution. The suspensions were shaken at 25°C and the residual Ag(I) concentration was monitored at different time interval by AAS.

2.5. Adsorption isotherm for Ag(I)

Adsorption isotherm was carried out by adding 20 mg adsorbent to a series of 20 mL Ag(I) solution with different

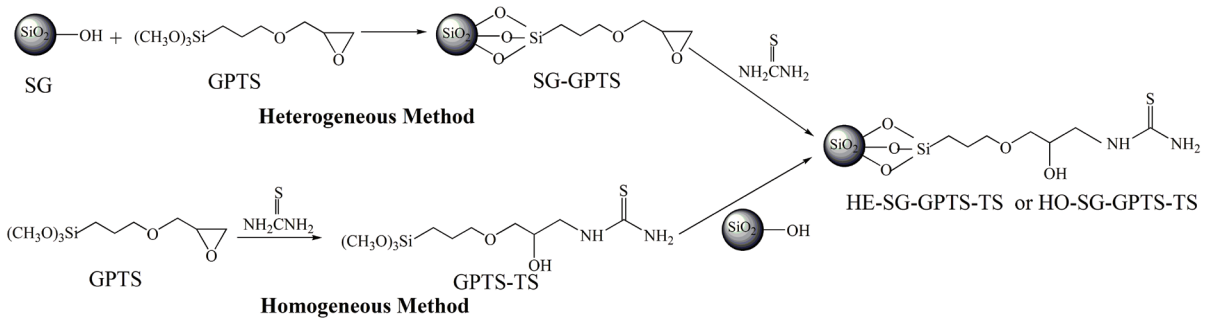

Fig. 1. Synthetic route for HO-SG-GPTS-TS and HE-SG-GPTS-TS.

concentration in the flasks. The mixtures were shaken for 12 h at 15°C, 25°C, and 35°C, respectively. After that, the concentration of Ag(I) was detected and the adsorption capacity was obtained.

2.6. Theoretical calculation on the adsorption isotherm

The adsorption mechanism was simulated by Gaussian 03 program by using density functional theory (DFT) method [28,29]. The surface functional group that bonded on silica gel was selected as the computational model and presented in Fig. 2. The geometry optimization was performed at B3LYP/6-31+G(d) (LANL2DZ for Ag(I)) level. After that, the interaction between functional group and Ag(I) was revealed on the basis of natural bond orbital (NBO) analysis at the level of B3LYP/6-311+G(d, p) (LANL2DZ for Ag(I)) [13].

3. Results and discussion

3.1. Saturated adsorption capacity

The saturated adsorption capacity of HO-SG-GPTS-TS and HE-SG-GPTS-TS for different metal ions is shown in Fig. 3. The adsorption capacity of HO-SG-GPTS-TS and HE-SG-GPTS-TS for metal ions follows the order of Ag(I) > Cu(II) > Pb(II) > Cd(II) > Mn(II) > Ni(II) > Co(II). The reason for this can be reasonable explained by the HSAB concept as sulfur containing functional group belongs to soft base, which exhibits remarkable binding ability toward metal ions that belong to soft acid, such as Hg(II), Ag(I), and Pd(II) [23].

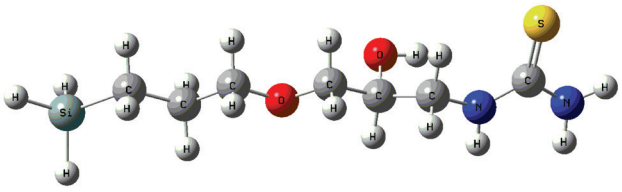

Fig. 2. Structure of the computational model.

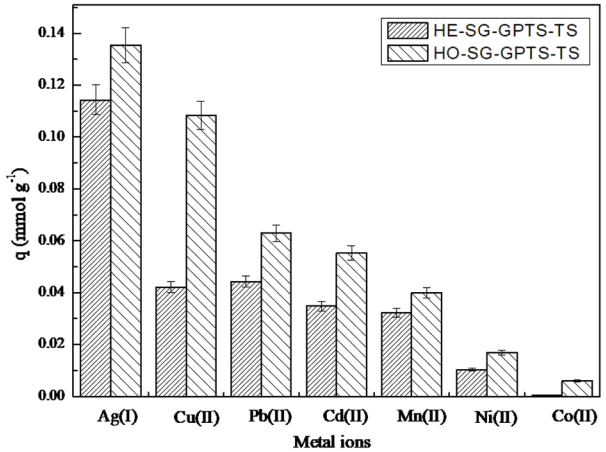

Fig. 3. Saturated adsorption capacity for metal ions for HO-SG-GPTS-TS and HE-SG-GPTS-TS adsorbents (Concentration: 0.002 mol·L^{-1}; pH: 6; temperature: 25°C and shaking time: 12 h).

Moreover, the borderline base of amino group also displays good affinity for Cu(II) that attributed to borderline acid, resulting in the relative higher adsorption capacity for Cu(II) than other metal ions. It can also observe the adsorption capacity of HO-SG-GPTS-TS is higher than HE-SG-GPTS-TS, suggesting homogeneous method is more efficient than heterogeneous method for the synthesis of adsorbent due to the high content of functional group provided by homogeneous method [27,30].

3.2. Effect of pH on the adsorption of Ag(I)

The effect of solution pH on the uptake of Ag(I) is presented in Fig. 4. It is clearly that the adsorption capacity is dramatically enhanced by the increase of pH, and the maximum adsorption is reached at pH 6. At low pH, the surface functional groups are existed in the protonation form, the positive charge impedes the contact of Ag(I) with the adsorbent, leading to the low adsorption capacity [27]. In addition, the competition between H^+ and Ag(I) also reduces the adsorption at low pH. With the increase of pH, both the protonation degree of functional groups and the competition between H^+ and Ag(I) decrease accordingly, which can provide more active binding sites, resulting in the increase of adsorption capacity. If the solution pH exceeds 6, the silver hydroxide maybe formed and hence this condition is undesired [31]. Therefore, pH 6 is selected for the following adsorption experiments.

3.3. Adsorption kinetic for Ag(I)

The adsorption kinetic curves for Ag(I) are depicted in Fig. 5. It is apparent that the adsorption of Ag(I) increases sharply during the first 120 min and then decreases until reach equilibrium at about 180 min. During the initial stage of the adsorption, the quick uptake of Ag(I) is mainly attributed to the abundant available binding sites of the adsorbent and

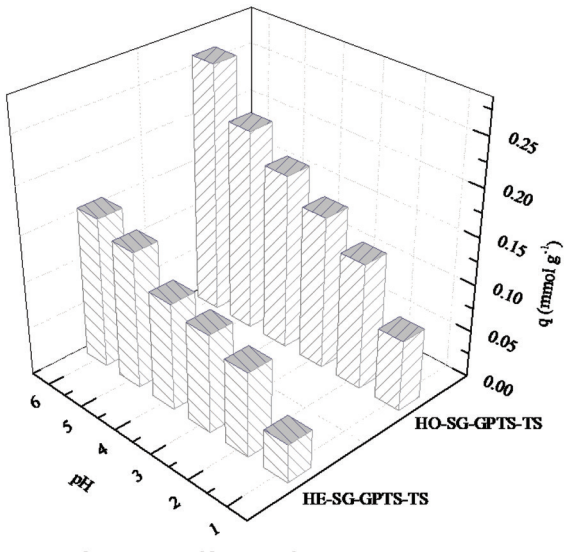

Fig. 4. Effect of pH on the adsorption of Ag(I) on HO-SG-GPTS-TS and HE-SG-GPTS-TS adsorbents (Concentration: 0.002 mol·L^{-1}; temperature: 25°C; and shaking time: 12 h).

high concentration of Ag(I), which facilitate the binding of Ag(I) with the adsorbent. With the adsorption proceeding, the number of available binding sites and Ag(I) concentration gradually decrease, resulting in the slowdown of the adsorption rate. The equilibrium adsorption capacity of HO-SG-GPTS-TS is also larger than HE-SG-GPTS-TS, further demonstrating the effectiveness of homogeneous method for the preparation of the adsorbent.

In order to evaluate the adsorption kinetic mechanism, pseudo-first-order and pseudo-second-order model that expressed by Eqs. (2) and (3) are employed to fit the kinetic data [32–35].

$$\ln(q_e - q) = \ln q_e - k_1 t \tag{2}$$

$$\frac{t}{q} = \frac{1}{k_2 q_e^2} + \frac{1}{q_e} t \tag{3}$$

where q_e and q are the amount of Ag(I) adsorbed at equilibrium and instantaneous time t (mmol·g^{-1}); k_1 (min^{-1}) and k_2 (g·mmol^{-1}·min^{-1}) are rate constants of pseudo-first-order and the pseudo-second-order model, respectively. The fitting results of are summarized in Table 1. It is clear that pseudo-second-order model displays superior fitness as compared with pseudo-first-order model with higher correlation coefficient (R_2^2). In addition, the calculated adsorption capacity ($q_{e,cal}$) obtained from pseudo-second-order model is closer to the experimental data ($q_{e,exp}$), further confirming the appropriateness of pseudo-second-order model to describe the adsorption kinetic for Ag(I).

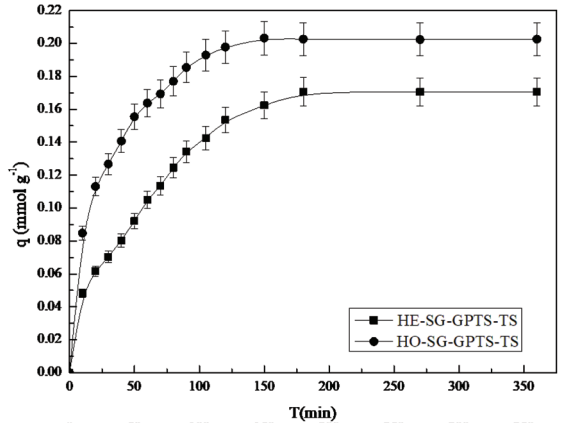

Fig. 5. Adsorption kinetic curves for Ag(I) on HO-SG-GPTS-TS and HE-SG-GPTS-TS adsorbents (Concentration: 0.002 mol·L^{-1}; pH: 6; and temperature: 25°C).

Boyed film diffusion model described by Eq. (4) is adopted to confirm whether film diffusion or intraparticle diffusion is the rate limiting step during the adsorption [36].

$$F = 1 - \frac{6}{\pi^2} \sum_{n=1}^{\infty} \frac{1}{n^2} \exp[-n^2 Bt] \tag{4}$$

where B represents time constant; n is an integer; and F is the fractional attainment which can be calculated by Eq. (5).

$$F = \frac{q_t}{q_e} \tag{5}$$

where q_e is the equilibrium adsorption capacity (mmol·g^{-1}), and q_t is the adsorption amount at time t (mmol·g^{-1}).

From the calculated F value, the corresponding Bt value can be obtained from the research of Reichenberg [37]. The rate limiting step can be distinguished through the fitting plots of Bt vs. t. When the fitting plot displays good linearity without passing through the origin, the adsorption is dominated by film diffusion. Otherwise, the adsorption will be controlled by intraparticle diffusion with the linear plot pass through the origin. The fitting linear equations of Bt vs. t and the corresponding parameters are presented in Table 2. As illustrated in Table 2, the plots exhibit excellent linearity without passing through the origin, proving the adsorption is controlled by film diffusion process.

3.4. Adsorption isotherm for Ag(I)

The adsorption isotherm of HO-SG-GPTS-TS and HE-SG-GPTS-TS for Ag(I) is presented in Fig. 6. The result reveals the adsorption capacity increases with the increase of metal ion concentration and temperature, which indicate high concentration gradient and temperature can promote the uptake of Ag(I). The isotherm data are simulated with Langmuir and Freundlich isotherm models. The linearized forms of the two models can be expressed by Eqs. (6) and (7) [6,38,39].

Table 2
Fitting parameters of Bt vs. t

Adsorbents	Linear equation	Intercept error	R^2
HE-SG-GPTS-TS	Bt = 0.0166t–0.3733	0.0603	0.9903
HO-SG-GPTS-TS	Bt = 0.0236t–0.1620	0.0633	0.9904

Table 1
Kinetic parameters for Ag(I) on HO-SG-GPTS-TS and HE-SG-GPTS-TS adsorbents

Adsorbents	$q_{e,exp}$ (mmol·g^{-1})	Pseudo-first-order kinetics			Pseudo-second-order kinetics		
		$q_{e,cal}$ (mmol·g^{-1})	k_1 (min^{-1})	R_1^2	$q_{e,cal}$ (mmol·g^{-1})	k_2 (mmol·g^{-1}·min^{-1})	R_2^2
HE-SG-GPTS-AP	0.17	0.20	0.0183	0.9930	0.19	0.1723	0.9948
HO-SG-GPTS-AP	0.20	0.14	0.0211	0.9938	0.22	0.2785	0.9980

$$\frac{C_e}{q_e} = \frac{C_e}{q_m} + \frac{1}{q_m K_L} \tag{6}$$

$$\ln q_e = \ln K_F + \frac{\ln C_e}{n} \tag{7}$$

where C_e is equilibrium concentration (mmol·mL^{-1}), q_e and q_m denote the equilibrium and maximum adsorption capacity (mmol·g^{-1}), K_L (mL·mmol^{-1}) and K_F (mmol·g^{-1}) represent the constant of the Langmuir and Freundlich models, and n is the intensity exponent.

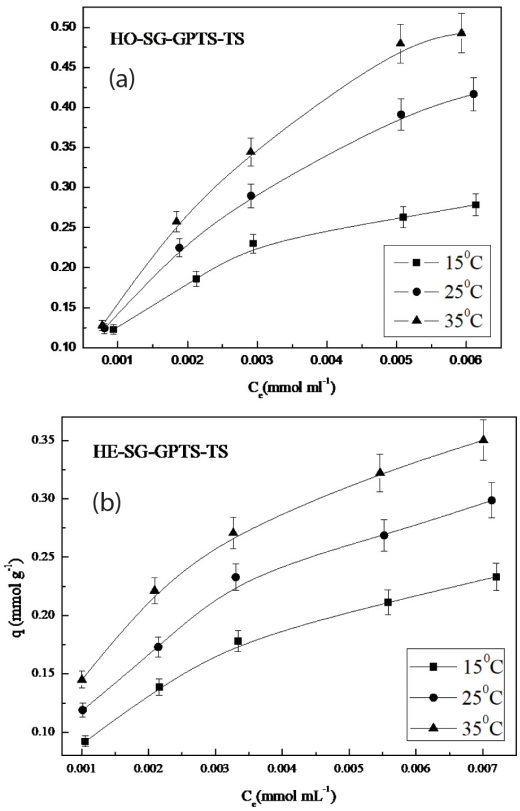

Fig. 6. Adsorption isotherm profiles for Ag(I) on (a) HO-SG-GPTS-TS and (b) HE-SG-GPTS-TS adsorbents (pH: 6; temperature: 25°C; and shaking time: 12 h).

The fitting parameters of Langmuir and Freundlich models are listed in Table 3. It is obvious the correlation coefficient (R^2) values obtained by Langmuir model are higher than the corresponding Freundlich model, suggesting Langmuir model is more suitable to fit the isotherm data and the adsorption proceeds by monolayer adsorption behavior. The comparison of q_m of HO-SG-GPTS-TS and HE-SG-GPTS-TS with alternative adsorbents is listed in Table 4. It is evident that HO-SG-GPTS-TS exhibits comparative higher adsorption capacity than the majority of the adsorbents, indicating HO-SG-GPTS-TS can be potentially used as efficient absorbent for the removal and recovery of Ag(I) from the aqueous solution.

D-R isotherm model is employed to distinguish whether the adsorption is physical or chemical in nature. The linear form of D-R model can be depicted as Eq. (8) [4,47].

$$\ln q_e = \ln q_m - \beta\varepsilon^2 \tag{8}$$

where β represents the activity coefficient (mol^2·kJ^{-2}), ε is the Polanyi potential which can be calculated from the following equation:

$$\varepsilon = RT \ln\left(1 + \frac{1}{C_e}\right) \tag{9}$$

Table 4
Comparison of q_m for Ag(I) with alternative adsorbents

Adsorbents	q_m (mmol·g^{-1})	References
HE-SG-GPTS-TS	0.40	This study
HO-SG-GPTS-TS	0.66	This study
Sulfoethyl functionalized silica	0.20	[40]
Clinoptilolites	0.29	[41]
Biochar	0.41	[42]
Raw vermiculite	0.43	[43]
Mesoporous silica	0.43	[44]
Thiourea-formaldehyde chelating resins	0.54	[45]
Bentonite clay	0.57	[12]
Thiol-functionalized Silica gel	0.70	[46]

Table 3
Adsorption isotherm parameters for Ag(I) at different temperatures for HO-SG-GPTS-TS and HE-SG-GPTS-TS

Metal ions	T (°C)	Langmuir			Freundlich		
		q_m (mmol·g^{-1})	K_L (mL·mmol^{-1})	R_L^2	K_F (mmol·g^{-1})	n	R_F^2
HE-SG-GPTS-AP	15	0.32	378.78	0.9974	2.59	2.05	0.9819
	25	0.40	390.68	0.9912	3.23	2.10	0.9779
	35	0.46	453.34	0.9991	3.37	2.23	0.9784
HO-SG-GPTS-AP	15	0.36	567.38	0.9981	2.62	2.32	0.9568
	25	0.66	275.62	0.9971	9.36	1.66	0.9902
	35	0.87	218.52	0.9921	16.49	1.49	0.9840

The mean free energy (E, kJ·mol^{-1}) of the adsorption can be derived from the value of β by Eq. (10).

$$E = \frac{1}{\sqrt{2\beta}} \tag{10}$$

The value of E can be used to evaluate the nature of the adsorption. The adsorption is physical in nature if E value below 8 kJ·mol^{-1}, while it is chemical in nature when the E value fall in the range of 8–16 kJ·mol^{-1} [4]. The fitting parameters of D-R model are summarized in Table 5, the E values are all in the range of 8–16 kJ·mol^{-1} at different temperature, indicating the uptake of Ag(I) was proceeded by chemical mechanism.

3.5. Thermodynamic parameters

Thermodynamic parameters including Gibbs free energy change (ΔG), enthalpy change (ΔH), and entropy change (ΔS) are calculated according to Eqs. (11) and (12) [4,28].

$$\ln K_L = \frac{\Delta S}{R} - \frac{\Delta H}{RT} \tag{11}$$

$$\Delta G = \Delta \mathrm{H} - T\Delta S \tag{12}$$

The calculated results are shown in Table 6. It can be seen that ΔG values are all negative, indicating the spontaneous nature of the adsorption. The positive values of ΔH suggest that the adsorption process for Ag(I) is endothermic. Moreover, the values of ΔS are all positive, which reveal the increase of entropy during the adsorption.

3.6. Theoretical calculation on the adsorption mechanism

The optimized geometries of Ag(I) complexes with functional group are presented in Fig. 7 and the relevant parameters are summarized in Table 7. It is evident that the functional group tends to coordinate Ag(I) by three modes during the adsorption. For Ag(I)-Complex-I, functional group behaviors as monodentate ligand to interact with Ag(I) by S atom, and the S-Ag bond length is 2.45 Å. For Ag(I)-Complex-II, the functional group coordinates with Ag(I) by S and hydroxyl O atoms to form bidentate complex. The bond lengths of S-Ag and O-Ag are 2.49 and 2.34 Å, respectively. Similar to Ag(I)-Complex-II, Ag(I)-Complex-III is also formed through two O atoms with the bond lengths of 2.28 and 2.40 Å.

NBO analysis are further performed to reveal the interaction and charge transfer between functional group and Ag(I) during the adsorption [13,29]. As can be seen from Table 7, NBO partial charges of Ag(I) in the complexes are all smaller than 1, while that of functional groups are all higher than 0. This indicates charge transfer from functional group to Ag(I) takes place during the adsorption. The transferred charges mainly spread to the 5s orbital of Ag(I), while a little portion distributes on the 5p and 6p orbitals. Second order perturbation theory analysis of Fock matrix in NBO basis is an effective tool to evaluate the interaction between donor atom and Ag(I) [28]. The stabilization energy E(2) between donor atom and metal ion can be used to confirm the contribution of donor atom during the adsorption. For Ag(I)-Complex-I, the E(2) for S and Ag(I) interaction is 3.24 kcal/mol, and is dominate by the electron transfer from lone pairs electron of S to the antibond empty orbital of S-Ag (LP(S)→BD*(Ag)). Different from Ag(I)-Complex-I, the σ donation of lone pair of electrons of S and O atoms to the empty orbital of Ag(I) dominates the formation of Ag(I)-Complex-II. The E(2) values of LP(S)→LP*(Ag) and LP(O)→LP*(Ag) are 35.18 and 10.88 kcal/mol, indicating S atom is the main contributor during the adsorption. Similar to Ag(I)-Complex-II, the E(2) values of LP(O)→LP*(Ag) are 4.62 and 10.07 kcal/mol for Ag(I)-Complex-III. The binding energy follow the order of Ag(I)-Complex-II > Ag(I)-Complex-III > Ag(I)-Complex-I, indicating the formation of Ag(I)-Complex-II by S and hydroxyl O atoms dominate the adsorption.

Table 6
Thermodynamic parameters for Ag(I) at different temperatures for HO-SG-GPTS-TS and HE-SG-GPTS-TS

Adsorbents	T (°C)	ΔG (kJ·mol^{-1})	ΔH (kJ·mol^{-1})	ΔS (J·mol^{-1}·K^{-1})
HE-SG-GPTS-TS	15	–14.27	6.63	72.18
	25	–14.89		
	35	–15.60		
HO-SG-GPTS-TS	15	–12.69	35.23	166.30
	25	–14.35		
	35	–16.02		

Table 5
Fitting parameters of D-R isotherm model

Adsorbents	T (°C)	Linear equation	q_m (mmol·g^{-1})	β (mol^2·J^{-2})	E (kJ·mol^{-1})	R^2
HE-SG-GPTS-TS	15	$Y = -7.15 \times 10^{-9}x - 0.43$	0.68	7.15×10^{-9}	8.36	0.9930
	25	$Y = -6.57 \times 10^{-9}x - 0.20$	0.81	6.57×10^{-9}	8.73	0.9867
	35	$Y = -5.80 \times 10^{-9}x - 0.09$	0.92	5.80×10^{-9}	9.28	0.9918
HO-SG-GPTS-TS	15	$Y = -6.29 \times 10^{-9}x - 0.31$	0.74	6.29×10^{-9}	8.92	0.9757
	25	$Y = -6.34 \times 10^{-9}x + 0.44$	1.55	6.34×10^{-9}	8.88	0.9981
	35	$Y = -6.56 \times 10^{-9}x + 0.79$	2.20	6.56×10^{-9}	8.73	0.9947

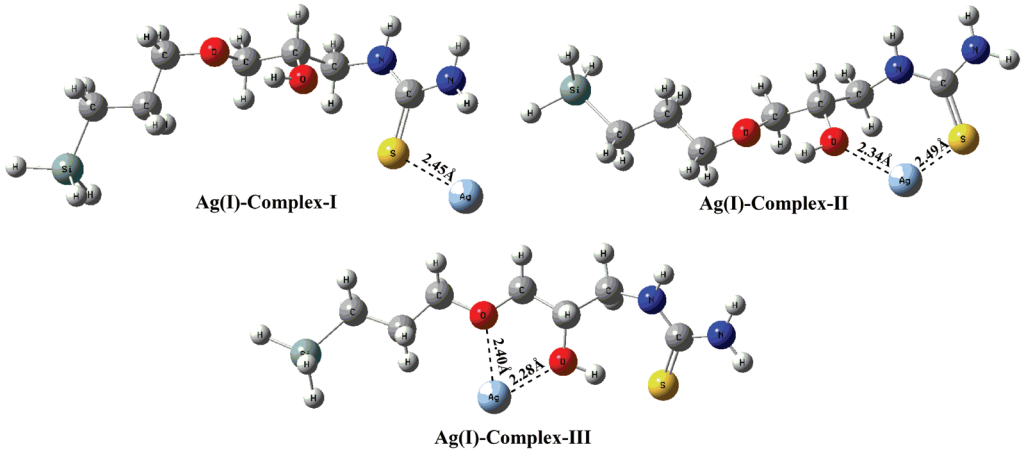

Fig. 7. Optimized geometries of Ag(I) complexes.

Table 7
Calculated parameters for the complexes

Complexes	Binding energy (kcal/mol)	NBO partial charge		Electron configuration of Ag(I)[a]
		Ligand	Ag(I)	
Ag(I)-Complexes-I	–571.48	0.28	0.72	$5s^{0.31}4d^{9.96}5p^{0.01}6p^{0.01}$
Ag(I)-Complexes-II	–582.97	0.24	0.76	$5s^{0.24}4d^{9.96}6p^{0.01}$
Ag(I)-Complexes-III	–571.49	0.10	0.90	$5s^{0.11}4d^{9.98}6p^{0.01}$

[a]Ground-state electron configurations of free Ag(I) is $4d^{10}$.

4. Conclusion

In this study, thiourea-functionalized silica gel (HO-SG-GPTS-TS and HE-SG-GPTS-TS) were synthesized and used for the removal of Ag(I) from aqueous solution. The effects of solution pH, contact time, temperature, and initial Ag(I) concentration on the adsorption were determined. Results show that the optimum adsorption pH is 6. Adsorption kinetic follows pseudo-second order model and is controlled by film diffusion process. The adsorption isotherm can be well described by monolayer Langmuir model and proceeds by chemical mechanism. Thermodynamic parameters suggest that the adsorption is a spontaneous, endothermic, and entropy increased process. DFT calculation reveals that the formation of chelates with Ag(I) by S and hydroxyl O atoms dominate the adsorption, and S is the main contributor. The charge transfer from functional group to Ag(I) takes place during the adsorption.

Acknowledgements

The authors are grateful for the financial support by the National Natural Science Foundation of China (21307053 and 21501087), Natural Science Foundation of Shandong Province (ZR2018MB039), Major Program of Shandong Province Natural Science Foundation (ZR2018ZC0946), Science and Technology Research Program of Yantai (2017ZH060), Major Program of Shandong Province Natural Science Foundation (ZR2018ZC0946), and The project of State Key Laboratory of Marine Coatings.

References

[1] L. Ma, Q. Wang, S. Islam, Y. Liu, S. Ma, M. Kanatzidis, Highly selective and efficient removal of heavy metals by layered double hydroxide intercalated with the MoS_4^{2-} Ion, J. Am. Chem. Soc., 138 (2016) 2858–2866.
[2] S. Lee, G. Barin, C. Ackerman, A. Muchenditsi, J. Xu, J. Reimer, S. Lutsenko, J. Long, C. Chang, Copper capture in a thioether-functionalized porous polymer applied to the detection of Wilson's disease, J. Am. Chem. Soc., 138 (2016) 7603–7609.
[3] J. Huang, Y. Li, Y. Cao, F. Peng, Y. Cao, Q. Shao, H. Liu, Z. Guo, Hexavalent chromium removal over magnetic carbon nanoadsorbents: synergistic effect of fluorine and nitrogen co-doping, J. Mater. Chem. A., 6 (2018) 13062–13074.
[4] J. Zhao, Y. Niu, B. Ren, H. Chen, S. Zhang, J. Jin, Y. Zhang, Synthesis of Schiff base functionalized superparamagnetic Fe_3O_4 composites for effective removal of Pb(II) and Cd(II) from aqueous solution, Chem. Eng. J., 347 (2018) 574–584.
[5] N. Singha, M. Karmakar, M. Mahapatra, H. Mondal, A. Dutta, M. Deb, M. Mitra, C. Roy, P. Chattopadhyay, An in situ approach for the synthesis of a gum ghatti-g-interpenetrating terpolymer network hydrogel for the high-performance adsorption mechanism evaluation of Cd(II), Pb(II), Bi(III) and Sb(III), J. Mater. Chem. A., 6 (2018) 8078–8100.
[6] H. Asiabi, Y. Yamini, M. Shamsayei, K. Molaei, M. Shamsipur, Functionalized layered double hydroxide with nitrogen and sulfur co-decorated carbondots for highly selective and efficient removal of soft Hg^{2+} and Ag^{+} ions, J. Hazard. Mater., 357 (2018) 217–225.
[7] T. Zhao, Y. Yao, D. Li, F. Wu, C. Zhang, B. Gao, Facile low-temperature one-step synthesis of pomelo peel biochar under air atmosphere and its adsorption behaviors for Ag(I) and Pb(II), Sci.Total. Environ., 640 (2018) 73–79.
[8] X. Liu, L. Yang, X. Luo, J. Pei, Y. Xi, C. Liu, L. Liu, A novel non-imprinted adsorbent with superior selectivity towards high-performance capture of Ag(I), Chem. Eng. J., 348 (2018) 224–231.

[9] W. Wei, A. Li, S. Pi, Q. Wang, L. Zhou, J. Yang, F. Ma, B. Ni, Synthesis of core-shell magnetic nanocomposite Fe_3O_4@ microbial extracellular polymeric substances for simultaneous redox sorption and recovery of silver ions as silver nanoparticles, ACS. Sustain. Chem. Eng., 6 (2018) 749–756.
[10] J. Kong, R. Gu, J. Yuan, W. Liu, J. Wu, Z. Fei, Q. Yue, Adsorption behavior of Ni(II) onto activated carbons from hide waste and high-pressure steaming hide waste, Ecotoxicol. Environ. Saf., 156 (2018) 294–300.
[11] S. Haider, F. Ali, A. Haider, W. Al-Masry, Y. Al-Zeghayer, Novel route for amine grafting to chitosan electrospun nanofibers membrane for the removal of copper and lead ions from aqueous medium, Carbohydr. Polym., 199 (2018) 406–414.
[12] M. Cantuaria, A. de Almeida Neto, E. Nascimento, M. Vieira, Adsorption of silver from aqueous solution onto pre-treated bentonite clay: complete batch system evaluation, J. Cleaner. Prod., 112 (2016) 1112–1121.
[13] P. Zhang, Y. Niu, W. Qiao, Z. Xue, L. Bai, H. Chen, Experimental and DFT investigation on the adsorption mechanism of silica gel supported sulfur-capped PAMAM dendrimers for Ag(I), J. Mol. Liq., 263 (2018) 390–398.
[14] S. Wan, W. Ding, Y. Wang, J. Wu, Y. Gu, F. He, Manganese oxide nanoparticles impregnated graphene oxide aggregates for cadmium and copper remediation, Chem. Eng. J., 350 (2018) 1135–1143.
[15] L. Fu, L. Zhang, S. Wang, J. Peng, G. Zhang, Selective adsorption of Ag^+ by silica nanoparticles modified with 3-Amino-5-mercapto-1,2,4-triazole from aqueous solutions, J. Mol. Liq., 241 (2017) 292–300.
[16] S. Benkhatou, A. Djelad, M. Sassi, M. Bouchekara, A. Bengueddach, Lead(II) removal from aqueous solutions by organic thiourea derivatives intercalated magadiite, Desal. Wat. Treat., 57 (2016) 9383–9395.
[17] Y. Niu, R. Qu, H. Chen, L. Mu, X. Liu, T. Wang, Y. Zhang, C. Sun, Synthesis of silica gel supported salicylaldehyde modified PAMAM dendrimers for the effective removal of Hg(II) from aqueous solution, J. Hazard. Mater., 278 (2014) 267–278.
[18] T. Abdel-Fattah, S. Haggag, M. Mahmoud, Heavy metal ions extraction from aqueous media using nanoporous silica, Chem. Eng. J., 175 (2011) 117–123.
[19] Y. Zhang, R. Qu, C. Sun, C. Ji, H. Chen, P. Yin, Improved synthesis of silica-gel-based dendrimer-like highly branched polymer as the Au(III) adsorbents, Chem. Eng. J., 270 (2015) 110–121.
[20] R. Taheri, N. Bahramifar, M. Zarghami, H. Javadian, Z. Mehraban, Nanospace engineering and functionalization of MCM-48 mesoporous silica with dendrimer amines based on 1,3,5-triazines for selective and pH-independent sorption of silver ions from aqueous solution and electroplating industry wastewater, Powder. Technol., 321 (2017) 44–54.
[21] M. Hong, X. Wang, W. You, Z. Zhuang, Y. Yu, Adsorbents based on crown ether functionalized composite mesoporous silica for selective extraction of trace silver, Chem. Eng. J., 313 (2017) 1278–1287.
[22] R. Randazzo, A. Di Mauro, A. D'Urso, G. Messina, G. Compagnini, V. Villari, N. Micali, R. Purrello, M. Fragala, Hierarchical effect behind the supramolecular chirality of silver(I)-cysteine coordination polymers, J. Phys. Chem. B, 119 (2015) 4898–4904.
[23] R.G. Pearson, Hard and soft acids and bases, J. Am. Chem. Soc., 85 (1963) 3533–3539.
[24] J. Yun, S. Bhattarai, Y. Yun, Y. Lee, Synthesis of thiourea-immobilized polystyrene nanoparticles and their sorption behavior with respect to silver ions in aqueous phase, J. Hazard. Mater., 344 (2018) 398–407.
[25] V. Losev, E. Elsufiev, O. Buyko, A. Trofimchuk, R. Horda, O. Legenchuk, Extraction of precious metals from industrial solutions by the pine (*Pinus sylvestris*) sawdust-based biosorbent modified with thiourea groups, Hydrometallurgy, 176 (2018) 118–128.
[26] K. Abbas, H. Znad, M. Awual, A ligand anchored conjugate adsorbent for effective mercury(II) detection and removal from aqueous media, Chem. Eng. J., 334 (2018) 432–443.
[27] Y. Niu, H. Liu, R. Qu, S. Liang, H. Chen, C. Sun, Y. Cui, Preparation and characterization of thiourea-containing silica gel hybrid materials for Hg(II) adsorption, Ind. Eng. Chem. Res., 54 (2015) 1656–1664.
[28] X. Song, Y. Niu, P. Zhang, C. Zhang, Z. Zhang, Y. Zhu, R. Qu, Removal of Co(II) from fuel ethanol by silica-gel supported PAMAM dendrimers: combined experimental and theoretical study, Fuel, 199 (2017) 91–101.
[29] M. Costa, L. Prates, L. Baptista, M. Cruz, I. Ferreira, Interaction of polyelectrolyte complex between sodium alginate and chitosan dimers with a single glyphosate molecule: A DFT and NBO study, Carbohydr. Polym., 198 (2018) 51–60.
[30] J. Chen, R. Qu, Y. Zhang, C. Sun, C. Wang, C. Ji, P. Yin, H. Chen, Y. Niu, Preparation of silica gel supported amidoxime adsorbents for selective adsorption of Hg(II) from aqueous solution, Chem. Eng. J., 209 (2012) 235–244.
[31] T. Wajima, Synthesis of zeolitic material from green tuff stone cake and its adsorption properties of silver (I) from aqueous solution, Microporous. Mesoporous. Mater., 233 (2016) 154–162.
[32] Y. Ho, Second-order kinetic model for the sorption of cadmium onto tree fern: a comparison of linear and non-linear methods, Water. Res., 40 (2006) 119–125.
[33] Y. Ho, G. McKay, Kinetic models for the sorption of dye from aqueous solution by wood, Process. Saf. Environ., 76 (1998) 183–191.
[34] Y. Ho, G. McKay, Sorption of dye from aqueous solution by peat, Chem. Eng. J., 70 (1998) 115–124.
[35] Y. Niu, R. Qu, C. Sun, C. Wang, H. Chen, C. Ji, Y. Zhang, X. Shao, F. Bu, Adsorption of Pb(II) from aqueous solution by silica-gel supported hyperbranched polyamidoamine dendrimers, J. Hazard. Mater., 244–245 (2013) 276–286.
[36] G. Boyd, A. Adamson, L. Myers, The exchange adsorption of ions from aqueous solutions by organic zeolites. II. Kinetics1, J. Am. Chem. Soc., 69 (1947) 2836–2848.
[37] D. Reichenberg, Properties of ion-exchange resins in relation to their structure. III. Kinetics of exchange, J. Am. Chem. Soc., 75 (1953) 589–597.
[38] X. Song, Y. Niu, Z. Qiu, Z. Zhang, Y. Zhou, J. Zhao, H. Chen, Adsorption of Hg(II) and Ag(I) from fuel ethanol by silica gel supported sulfur-containing PAMAM dendrimers: kinetics, equilibrium and thermodynamics, Fuel, 206 (2017) 80–88.
[39] A. Selim, E. Mohamed, M. Mobarak, A. Zayed, M. Seliem, S. Komarneni, Cr(VI) uptake by a composite of processed diatomite with MCM-41: isotherm, kinetic and thermodynamic studies, Microporous. Mesoporous. Mater., 260 (2018) 84–92.
[40] L. Zhang, G. Zhang, S. Wang, J. Peng, W. Cui, Sulfoethyl functionalized silica nanoparticle as an adsorbent to selectively adsorb silver ions from aqueous solutions, J. Taiwan. Inst. Chem. E., 71 (2017) 330–337.
[41] S. Çoruh, G. Şenel, O. Ergun, A comparison of the properties of natural clinoptilolites and their ion-exchange capacities for silver removal, J. Hazard. Mater., 180 (2010) 486–492.
[42] E. Antunes, M. Jacob, G. Brodie, P. Schneider, Silver removal from aqueous solution by biochar produced from biosolids via microwave pyrolysis, J. Environ. Manage., 203 (2017) 264–272.
[43] A. Sarı, M. Tüzen, Adsorption of silver from aqueous solution onto raw vermiculite and manganese oxide-modified vermiculite, Microporous. Mesoporous. Mater., 170 (2013) 155–163.
[44] H. Yang, R. Xu, X. Xue, F. Li, G. Li, Hybrid surfactant-templated mesoporous silica formed in ethanol and its application for heavy metal removal, J. Hazard. Mater., 152 (2008) 690–698.
[45] S. Kirci, M. Guelfen, A. Aydin, Separation and recovery of silver(I) ions from base metal ions by thiourea- or urea-formaldehyde chelating resin, Sep. Sci. Technol., 44 (2009) 1869–1883.
[46] D. Quang, J. Lee, J. Kim, Y. Kim, G. Shao, H. Kim, A gentle method to graft thiol-functional groups onto silica gel for adsorption of silver ions and immobilization of silver nanoparticles, Powder. Technol., 235 (2013) 221–227.
[47] M. Mahmoud, G. Nabil, H. Abdel-Aal, N. Fekry, M. Osman, Imprinting "Nano-SiO_2-crosslinked chitosan-nano-TiO_2" polymeric nanocomposite for selective and instantaneous microwave-assisted sorption of Hg(II) and Cu(II), ACS. Sustain. Chem. Eng., 6 (2018) 4564–4573.